ATLANTIS PRESS
Advances in Engineering Research, volume 103
Proceedings of the 3rd International Conference on Material Engineering and Application (ICMEA 2016)

Electrospun Composite of Fe_3o_4/Cu Nanocrystals Encapsulated in Carbon Fibers as an Anode Material with High Rate Capability for Lithium Ion Batteries

Meng ZHANG[1,a], Jing WANG[1,2, b*], Shi CHEN[1,2,c] and Feng WU[1,2,d]

[1]School of Materials Science and Engineering, Beijing Key Laboratory of Environmental Science and Engineering, Beijing Institute of Technology, Beijing, 100081, China

[2]Collaborative Innovation Center of Electric Vehicles in Beijing, Beijing, 100081, China

[a]wushengqingzhu@163.com,[b]wangjingbit98@bit.edu.cn, [c]csbit@bit.edu.cn, [d]wufeng863@bit.edu.cn

*Corresponding author

Keywords: Magnetite, Metallic Cu, Fibrous Structure, Anode, Lithium Ion Batteries.

Abstract: In this paper, a new composite with Fe_3O_4 and Cu nanoparticles encapsulated in carbon nanofibers (CNFs) and its electrochemical properties were reported. The composite is fabricated by a simple electrospinning technique followed by heat treatment. At a current density of 100 mA g^{-1}, this electrode exhibits a high reversible capacity of 540.5 mAh g^{-1} after 100 cycles. Moreover, this composite electrode also shows good rate capability when current density increased from 0.1 to 5.0 Ag^{-1}.This excellent performances can be ascribed to the novel fiber architecture and Cu introduction. Cu nanocrystal in the CNFs ensures the composite a good conductive ability.

Introduction

In recent years, rechargeable lithium-ion batteries (LIBs) have been intensively used in clean energy storage, especially portable electronics[1]. However, there is a pressing challenge to develop more advanced LIBs for satisfying the application demands in electric vehicles (EVs) [2]. At present, commercial graphite anode because of its theoretical limit (372mAh g^{-1}) is difficult to meet the higher capability requirement of LIBs for EV. Many transition metal oxides (MO_x, M: Fe, Sn, Cu, etc.)[3-5] have been involved in the development of LIBs anodes materials due to their higher specific capacities. As a promising anode, Ferriferous oxide (Fe_3O_4) has attracted comprehensive attention on the basis of its high theoretical capacity of 924 mAh g^{-1}, relatively low-cost and good electrochemical activity [6]. However, the large volume expansion (93%) during charge/discharge and the low conductivity for Fe_3O_4 are messy problems for power battery application demands in capacity and good cycling stability [7].

In order to overcome the above complex problems, downsizing various Fe_3O_4-based materials is one of promising approaches to the mechanical instabilities of Fe_3O_4. Firstly, various carbon material (nanofiber, nanotube, graphene, etc) is usually exploited as a matrix to load Fe_3O_4 nanoparticles, taking full advantage of physical stability and electrical conductivity [8, 9]. Secondly, the excellent conductive metals (Ag, Cu,) have been introduced, which can significantly increases the rate performance of material.

Herein, we tried to design a composite with Fe_3O_4 and Cu nanocrystals (5.96×10^7 S m^{-1}) encapsulated in CNFs by a simple electrospinning technique and heat treatment, which can merge the characteristics of CNF and Cu to enhance the electrochemical performance of the Fe_3O_4-based anode. The detailed synthesis process of the composite is illuminated in Fig. 1. In this synthesis, $Fe(NO_3)_3$ and $Cu(CH_3COO)_2$ will be simultaneously implanted into Polyvinyl Pyrrolidone (PVP) fibers by electrospinning. By the followed heat treatment, Fe_3O_4 and Cu particles may generate in situ in the carbonized nanofibers. The structure and morphologies of the composite are discussed in detail.

Copyright © 2016, the Authors. Published by Atlantis Press.
This is an open access article under the CC BY-NC license (http://creativecommons.org/licenses/by-nc/4.0/).

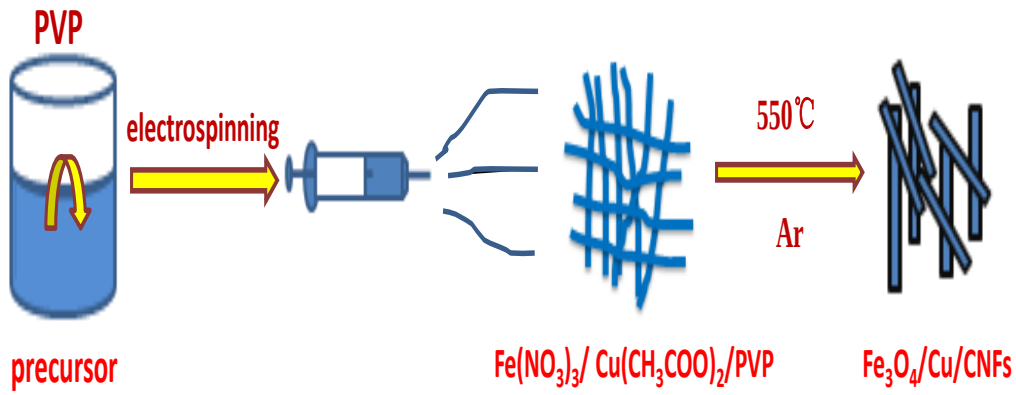

Fig. 1 Schematic illustration of the formation process of the Fe_3O_4 /Cu/CNFs composite

Experimental

Material Preparation

All the reagents were analytical grade without further purification. Polyvinyl Pyrrolidone (PVP, M_w=1 300 000, Aladdin) was used to fabricate the precursor fibers. $Cu(CH_3COO)_2 \cdot 2H_2O$ and $Fe(NO_3)_3 \cdot 9H_2O$ were purchased from Beijing Chemical Works.

Electrospinning solution was prepared by dissolving 1g PVP in 10mL N, N-dimethylformamide (DMF) with stirring at 40℃ for 1h. Then, 0.8 g of $Fe(NO_3)_3 \cdot 9H_2O$ and 0.2 g of $Cu(CH_3COO)_2 \cdot 2H_2O$ was added to the resulting solution with further stirring at 40℃ for 12 h. The obtained solution was added in a 10 ml syringe with stainless steel needles. For the electrospinning (SS-2534, Beijing Ucalery Company), a high voltage of 15 kV and flow rate of 0.5mL/h were adopted, and the needle-to-collector distance was 14 cm. After electrospinning process, the electrospun PVP/$Fe(NO_3)_3$/ $Cu(CH_3COO)_2$ fibers were peeled off from the collector and dried in a vacuum oven at 80℃ for 12 h. This sample was carbonized at 550℃ for 2 h under argon atmosphere with a heating rate 5℃min^{-1}. Fe_3O_4/CNFs and CNFs composites were also fabricated using the similar process.

Characterization

Scanning electron microscope (FEI QUANTA 6000) and high-resolution transmission electron microscope (HR-TEM, FEI TECNAIG2 F30) were used to investigate the morphologies and microstructure of Fe_3O_4/Cu/CNFs and their precursor fibers. The crystal structure was measured by X-ray diffraction using an Ultima IV diffractometer with Cu Ka radiation at a scan rate of 8 °min^{-1} from 10 °to 90 °.

Electrochemical Characterization

The working electrodes consisted of active materials (Fe_3O_4/Cu/CNFs, Fe_3O_4 and CNFs), conductive agent (acetylene black) and binder (poly vinylidene fluoride) (8 : 1 : 1 in weight ratio), which were dissolved in methyl pyrrolidinone to form a viscous slurry. The above slurry was coated on a copper foil and dried in the vacuum oven at 80℃for 12h to form electrode film. CR2025 coin half-cells were assembled in an Ar-filled glove box , in which moisture and oxygen levels were less than 1 ppm using lithium foils as the counter electrode and Celgard 2300 film as the separator The electrolyte was 1mol L^{-1} $LiPF_6$/DMC + DEC + EC solution (1 : 1 : 1 in volume). Galvanostatic charge–discharge tests of the cells were measured by a Land 2001A CT battery tester (vs Li^+/Li). Cyclic voltammetry (CV) of the electrode was measured at a scan rate of 0.1 mV s^{-1} within the range of 0.01–3.00 V. Electrochemical impedance spectroscopy (EIS) was performed on an electrochemical workstation (CHI 660C) under the frequency range from 100 kHz to 10 mHz.

Results and Discussion

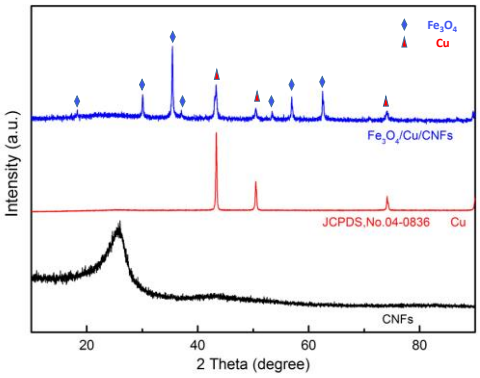

Fig. 2 (a) XRD patterns of CNFs, Cu and Fe_3O_4/Cu/CNFs composite.

In order to compare crystal structure and phase composition, the patterns of Fe_3O_4/Cu/CNFs, pure Fe_3O_4 and Cu determined by XRD are shown in Fig.2. In the pattern of CNFs, there are two broad peaks at 2θ= 26 º and 43 º, implying the (002) and (100) planes of carbon with a non-graphitized structure[10]. The peaks appearing at 2θ = 18.3, 30.1, 35.4, 37.1, 43.0, 47.1, 53.4, 56.9, 62.5, 70.9, 73.9 and 86.7 º correspond to the cubic phase of Fe_3O_4 with the planes of (111), (220), (311), (222), (400), (422), (511), (440), (620), (533) and (642)[11]. Respectively, all of the reflection peaks for both raw Fe_3O_4 and Fe_3O_4/Cu/CNFs can be indexed to face-centered-cubic magnetite Fe_3O_4 (JCPDS, no. 99-0073). The obviously high background of composite in the XRD pattern indicates the presence of amorphous carbon[9]. Besides, the diffraction peaks of metallic Cu at 43.3, 50.4 and 74.1 º are indexed to the (111), (200) and (220) planes (JCPDS, no. 04-0836)[12]. These study results demonstrate the composite fibers comprised of Fe_3O_4, Cu and carbon phases have been successful prepared by electrospinning and subsequent treatment.

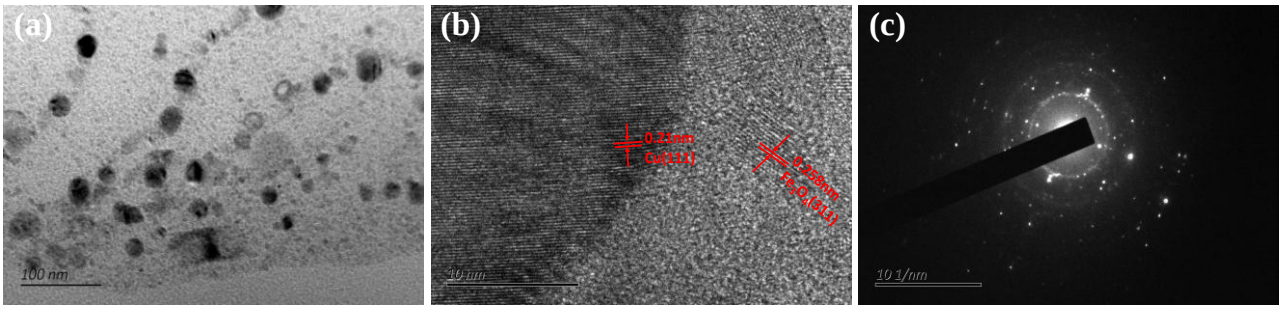

Fig. 3 (a, b) HRTEM images of Fe_3O_4/Cu/CNFs composite, (c) FFT pattern of Fe_3O_4/Cu/CNFs composite.

Fig. 3a and 3b show TEM images of Fe_3O_4/C composite architecture. Clearly, the uniform Fe_3O_4 and Cu crystals are homogeneously embedded in the CNFs without apparent agglomeration. The particle size has an average diameter of ~15−30 nm, which is well consistent with the calculated result from Scherrer's formula. The HRTEM image in Figure 3b demonstrates a typical Fe_3O_4 particle with good crystalline texture. The d-spacings of 0.258 nm are in good consistent with the (311) planes[13], respectively. Besides, the well-resolved lattice fringe distance of 0.21 nm can be indexed to the (111) plane of single-crystalline Cu[14]. The ambient phase exhibiting an amorphous structure is good agreement with the carbon host.

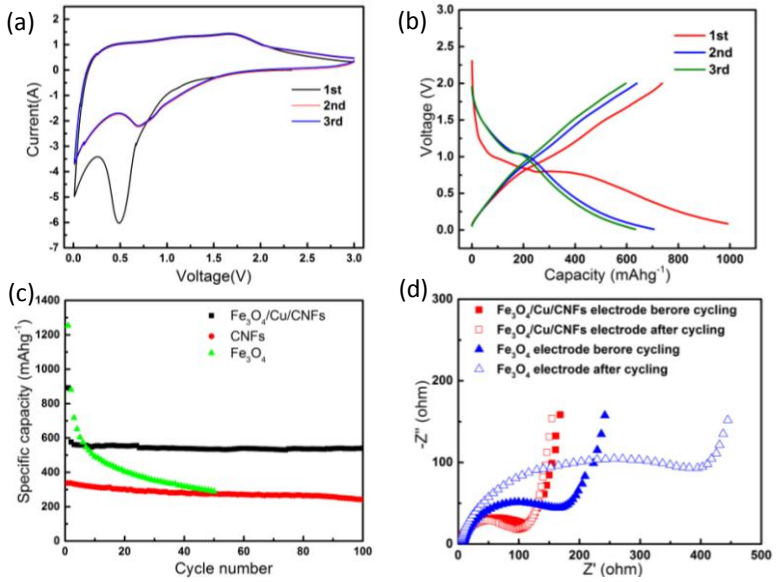

Fig. 4 Electrochemical performance of Fe_3O_4/Cu/CNFs anodes
(a) CVs of Fe_3O_4/Cu/CNFs anode (0.1 mV s^{-1})
(b) Discharge/charge profiles of Fe_3O_4/Cu/CNFs anodes cycled between 0.01 and 2.0 V at a current density of 100mA g^{-1}
(c) Cycling performances of Fe_3O_4/Cu/CNFs, pure Fe_3O_4, and CNFs anodes at 100mAg^{-1}
(d) Impedance spectra of Fe_3O_4@PCF anode before cycling and after cycling respectively

The electrochemical measurements of Fe_3O_4/Cu/CNFs composite anode are presented in Fig. 4. Fig. 4a shows the cyclic voltammograms curves of Fe_3O_4/Cu/CNFs composite electrode at a scan rate of 0.1 mVs^{-1}. An obvious cathodic peak is observed during the first cycle at the potential of 0.5V in the first cathodic curve, which can be attributed to the electrochemical lithiation process of Fe_3O_4 and the formation of solid electrolyte interphase (SEI).

$$Fe_3O_4 + 2Li^+ + 2e^- \rightarrow Li_2(Fe_3O_4) \quad (1)$$

$$Li_2(Fe_3O_4) + 6Li^+ + 6e^- \rightarrow 3Fe^0 + 4Li_2O \quad (2)$$

$$3Fe^0 + 4Li_2O \rightarrow Fe_3O_4 + 2Li^+ + 2e^- \quad (3)$$

From the 2nd CV cycle, a cathodic peak observed at 0.69 corresponds to the reduction reaction (eq 2 and 3), which indicates that a stable SEI film has been formed on the surface of carbon shell during the first cycle. In the first anodic half-cycles, the anodic peak at 1.75 V corresponds to the oxidation process of Fe^0 to Fe_3O_4 (eq 3). The CV curves from the 2nd cycle with no apparent shift indicates that the Fe_3O_4/Cu/CNFs electrode shows an excellent reversibility during charge and discharge processes[15].The discharge/charge profiles of Fe_3O_4/Cu/CNFs between 0.01 and 2.0 V for different cycles at a current density of 100mA g^{-1} are shown in Fig. 4b. In the first lithiation and delithiation process, the bare Fe_3O_4 electrode shows a specific capacity of 1216.3 and 879.5 mAh g^{-1} with a Coulombic efficiency of 72.3%. It is noted that there are two voltage plateaus at 1.0 V and 0.7 V in the first discharge cycle, but only one plateau at 0.8 V in the subsequent cycles, which are good agreement with the cathodic and anodic peaks in the 1st CV curve (Fig. 4a).

The cycling performance of the Fe_3O_4/Cu/CNFs, pure Fe_3O_4, composite electrode at a current density of 100 mAg^{-1} are shown in Fig. 4c. The initial discharge capacity of pure Fe_3O_4 electrode decreasing from 1318 to 292 mAh g^{-1} after 50 cycles shows a rapid fading trend. During the cycling process, because of the large volume change of Fe_3O_4 and direct contact with the electrolyte, the SEI would be destroyed and formed repeatedly leading to a poor cycling performance [16]. Compared with the pure Fe_3O_4 NPs, The Fe_3O_4/Cu/CNFs composite electrode keeps a high discharge capacity of 540.5 mAh g^{-1} after 100 cycles, which is more than the value of CNFs (371.4

mAh g^{-1}) under the same experimental conditions. The superior capacity stability of Fe_3O_4/Cu/CNFs can be mainly attributed to the designed hierarchical structure, where active particles are implanted into carbon framework. This novel structure is helpful to block solvents of electrolyte and prevent the active material from agglomeration and pulverization upon continuous cycling.

In order to investigate the changes of electrical conductivity, EIS measurements are measured for Fe_3O_4/Cu/CNFs and Fe_3O_4 electrode before and after cycling (Fig. 4d). All the three Nyquist plots contain one semicircle at high frequencies attributed to a charge-transfer phenomenon, and an inclined line at low frequencies ascribed to the mass-transfer process[17]. It is noted that the charge transfer resistance (R_{ct}) of the Fe_3O_4/Cu/CNFs electrode is 112Ω for the fresh cell, which is apparently smaller than that of the pure Fe_3O_4 electrode (163 Ω). This comparison means the composite electrode has a stronger electrochemical reactivity and higher charge-transfer rate. After charge–discharge for 100 cycles, its charge transfer resistance decreases to 88.3Ω, which may be due to more sufficient contact between active materials and the electrolyte in this case. On the contrary, the resistance Rct of bare Fe_3O_4 electrodes increases dramatically after 100 cycles from 163.8 to 395 Ω. This phenomenon may be ascribed to electrode degradation after long cycles of lithiation/delithiation.

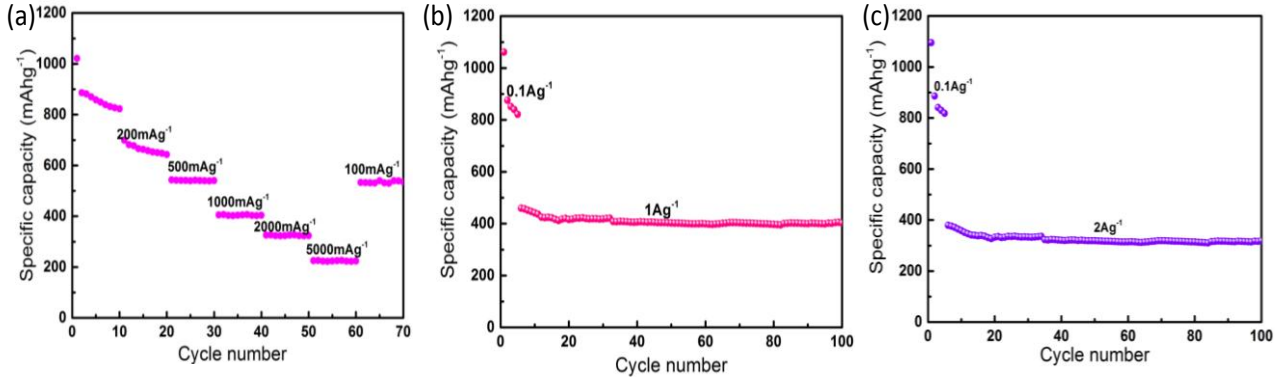

Fig. 5 (a) Rate performance of the Fe_3O_4/Cu/CNFs composite at various current densities, (b) (c) cycling performance of the Fe_3O_4/Cu/CNFs composite at current densities of 1.0 and 2.0 A g-1

The excellent rate capability of the Fe_3O_4/Cu/CNFs composites was showed in Fig. 5a. When the current densities increases from 0.2 to 0.5, 1.0, 2.0 and 5.0 A g^{-1}, Fe_3O_4/Cu/CNFs composites deliver a reversible capacity of 620, 548.8, 405, 325.8, 195 mAh g^{-1}, respectively. After the high-rate test, the reversible capacity of Fe_3O_4/C electrode will recover to 530.8 mAh g^{-1} at 100 mAh g^{-1}. Besides, when the current densities are 1000 and 2000 mA g^{-1}, it exhibits 405 and 331.5 mAh g^{-1} reversible capacities after 100 cycles, respectively (Fig. 5b, 5c). The superior rate capacity may be attributed to the implanted Cu and one-dimensional structure CNFs support. Metallic Cu possessing a high conductivity is helpful to improving the electrical the Composite material conductivity.

Conclusions

In summary, we synthesized successfully a novel Fe_3O_4/Cu/CNFs composite by a simple electrospinning method and subsequent carbonization. Fe_3O_4 and Cu particles were embedded controllably in carbon framework without apparent agglomeration. The composite electrode shows superior electrochemical properties with high specific capacities, long cycling life and excellent rate performance. This superior performance, especially the rate capability, is mainly attributed to dispersed Fe_3O_4 and Cu nanocrystals and one-dimensional structural CNFs which make a significant contribution to reduce the Li ions transport pathway. Besides, the introduced metallic Cu plays a huge role in the modification of the rate performance.

Acknowledgments

This work was financially supported by the National Key R&D Program (Grant No. 2016YFB0100400). We also thank the support from the Special fund of Beijing Co-construction Project.

References

[1] M. Armand, J.-M. Tarascon, Building better batteries, Nature. 451 (2008) 652-657.

[2] B. Dunn, H. Kamath, J.-M. Tarascon, Electrical energy storage for the grid: a battery of choices, Science. 334 (2011) 928-935.

[3] M. Reddy, G. Subba Rao, B. Chowdari, Metal oxides and oxysalts as anode materials for Li ion batteries, Chem. Rev. 113 (2013) 5364-5457.

[4] X. Guan, J. Nai, Y. Zhang, CoO hollow cube/reduced graphene oxide composites with enhanced lithium storage Capability, Chem. Mater. 26 (2014) 5958-5964.

[5] X. Sun, W. Si, X. Liu, Multifunctional Ni/NiO hybrid nanomembranes as anode materials for high-rate Li-ion batteries, Nano Energy. 9 (2014) 168-175.

[6] H.B. Wu, J.S. Chen, H.H. Hng, Nanostructured metal oxide-based materials as advanced anodes for lithium-ion batteries, Nanoscale. 4 (2012) 2526-2542.

[7] S.H. Lee, S.H. Yu, J.E. Lee, Self-Assembled Fe_3O_4 nanoparticle clusters as high-performance anodes for lithium ion batteries via geometric confinement, Nano letters. 13 (2013) 4249-4256.

[8] P. Wang, M. Gao, H. Pan, A facile synthesis of Fe_3O_4/C composite with high cycle stability as anode material for lithium-ion batteries, J. Power Sources. 239 (2013) 466-474.

[9] Z. Zeng, H. Zhao, J. Wang, Nanostructured Fe_3O_4@C as anode material for lithium-ion batteries, J. Power Sources. 248 (2014) 15-21.

[10] L. Qie, W.M. Chen, Nitrogen-doped porous carbon nanofiber webs as anodes for lithium ion batteries with a superhigh capacity and rate capability, Adv. Mater. 24 (2012) 2047-2050.

[11] F. Wu, R. Huang, D. Mu, New synthesis of a foamlike Fe_3O_4/C composite via a self-expanding process and its electrochemical performance as anode material for lithium-ion batteries, ACS Appl. Mater. Interfaces. 6 (2014) 19254-19264.

[12] F.F. Cao, J.W. Deng, S. Xin, Cu-Si nanocable arrays as high-rate anode materials for Lithium-ion batteries, Adv. Mater. 23 (2011) 4415-4420.

[13] S. Gu, Y. Liu, G. Zhang, Fe_3O_4/carbon composites obtained by electrospinning as an anode material with high rate capability for lithium ion batteries, RSC Adv. 4 (2014) 41179-41184.

[14] C.S. Choi, Y.-U. Park, H. Kim, Three-dimensional sponge-like architectured cupric oxides as high-power and long-life anode material for lithium rechargeable batteries, Electrochimica Acta. 70 (2012) 98-104.

[15] C. He, S. Wu, N. Zhao, Carbon-encapsulated Fe_3O_4 nanoparticles as a high-rate lithium ion battery anode material, ACS nano. 7 (2013) 4459-4469.

[16] N. Zhao, S. Wu, One-pot synthesis of uniform Fe_3O_4 nanocrystals encapsulated in interconnected carbon nanospheres for superior lithium storage capability, Carbon. 57 (2013) 130-138.

[17] T.H. Hwang, Y.M. Lee, B.-S. Kong, Electrospun core–shell fibers for robust silicon nanoparticle-based lithium ion battery anodes, Nano letters. 12 (2012) 802-807.